Supporting Information for

Copper(I) / $NO_{(g)}$ Reductive Coupling Producing a *trans*-Hyponitrite Bridged Dicopper(II) Complex – Redox Reversal Giving Copper(I) / $NO_{(g)}$ Disproportionation

Gayan B. Wijeratne, Shabnam Hematian, Maxime A. Siegler, and Kenneth D. Karlin*

Department of Chemistry, Johns Hopkins University, Baltimore, Maryland 21218, United States

CONTENTS

1. Materials and Methods

All commercially available chemicals were purchased at the highest available purity, and used as received unless otherwise stated. Synthesis and manipulation of air-/moisture-sensitive substances were carried out using standard Schlenk techniques under an argon atmosphere, or in a nitrogen-filled Vacuum Atmospheres OMNI-LAB glovebox with H_2O and O_2 levels <1 ppm. All organic solvents were purchased at HPLC-grade or better. Methanol and DCM were degassed (bubbling argon gas for 20 min at room temperature) and dried (passing through a 60 cm alumina column) using an Innovative Technologies (2003) solvent purification system (model: sps-400-6). THF was distilled over sodium benzophenone, and MeCN over calcium hydride under an argon atmosphere prior to use. All solvents were further degassed by passing argon gas for 40-50 min in an addition funnel connected to an evacuated Schlenk flask under an inert atmosphere. These solvents were then stored in dark glass bottles inside the glovebox over 3 or 4 Å molecular sieves at least for 72 hrs. Nitric oxide was purchased from Matheson Gases and purified according to published procedures.[1-3] Purified $NO_{(g)}$ was then stored in 25 or 50 mL Schlenk flasks sealed with a rubber septum and copper wire. Dioxygen was dried by passing through a short column of drierite prior to use. Semi-quantitative QUANTOFIX nitrite test strips were purchased from Sigma Aldrich. UV-Vis absorption spectra were collected on a Carey-50 Bio spectrometer coupled to a UnispeKs CoolSpeK cryostat (Unisoku Scientific Instruments), where the sample temperature was controlled in a10 mm path length quartz Schlenk cuvette. Infrared (IR) vibrational spectra were collected on a Thermo Scientific Nicolet Nexus 670 Fourier transform spectrometer. Electron paramagnetic resonance (EPR) spectra were collected in 5 mm (outer diameter) quartz tubes using an X-band Bruker EMX-plus spectrometer coupled to a Bruker ER 041 XG microwave bridge (Experimental conditions: microwave frequency = 9.41 GHz; microwave power = 0.2 mW; modulation frequency = 100 kHz; modulation amplitude = 10 G; temperature = 20 K) EPR simulations were performed using EasySpin 5.1.12 and MATLAB R2017a. Gas chromatographic analysis for headspace $N_2O_{(g)}$ quantification was carried out using a Varian CP-3800 instrument (manual injection) equipped with a 25 m 5 Å molecular sieve capillary column, and an electron capture detector. These GC samples were injected using a 100 µL gas-tight syringe, and the injector oven and detector oven were maintained at 200 and 300 ^oC, respectively. The GC column temperature was set at 150 ^oC. The duration of each GC experiment was 10 min. Crystallographic data collection was performed on a SuperNova X-ray diffractometer (Agilent Technologies) at Johns Hopkins University. Elemental analysis was conducted by Micro-analysis Inc., Wilmington, DE. The syntheses of TMPA ligand,[4] $[Cu^{I}(MeCN)_4][B(C_6F_5)_4]$,[5] $[Cu^{II}(tmpa)Cl](ClO_4)$,[6] $[Cu^{II}(tmpa)(MeCN)](ClO_4)_2$,[7] $[Cu^{I}(tmpa)(MeCN)][B(C_6F_5)_4]$,[6] $[Cu^{II}(tmpa)(NO_2)][B(C_6F_5)_4]$,[6] *trans*-$Ag_2N_2O_2$,[8] and *trans*-$H_2N_2O_2$[8] were carried out according to previously published methods.

2. Synthesis of $[\{Cu^{II}(tmpa)\}_2(\mu\text{-}N_2O_2^{2-})]^{2+}$ from $[Cu^{I}(tmpa)(MeCN)]^{+}$ and $NO_{(g)}$

The addition of excess nitric oxide ($NO_{(g)}$) to $[Cu^{I}(tmpa)(MeCN)][B(C_6F_5)_4]$ in MeOH resulted in the formation of $[\{Cu^{II}(tmpa)\}_2(\mu\text{-}N_2O_2^{2-})]^{2+}$ in high (>97%) yields. The detailed procedure is as follows: A 1 mM MeOH solution of $[Cu^{I}(tmpa)(MeCN)][B(C_6F_5)_4]$ (2.2 mg, 2×10^{-3} mmol) was placed in a 10 mm path length Schlenk cuvette, and electronic absorption spectral changes were monitored at room temperature, as purified nitric oxide was added in by means of a three-way syringe as described earlier.[6] New features grew in at λ_{max} = 310 (ε = 3800 M^{-1} cm^{-1}), 675 (ε = 250 M^{-1} cm^{-1}), and 870 (ε = 340 M^{-1} cm^{-1}) nm immediately after the addition of $NO_{(g)}$, as the solution color changed from pale yellow to deep green (Figure 2; main text). These absorption features are in sheer contrast to those of the $[Cu^{II}(tmpa)(NO_2)]^{+}$ species, the major solution product expected from the previously observed[9] Cu^{I}-mediated $NO_{(g)}$-disproportionation. The MeOH reaction was repeated at a 100 mg scale in order to generate bulk material for characterization. The final product was further characterized by EPR spectroscopy (Figure S1) and elemental analysis. EPR g- and A-values when compared with those of $[Cu^{II}(tmpa)(NO_2)]^{+}$ clearly indicates the formation of the new $[\{Cu^{II}(tmpa)\}_2(\mu\text{-}N_2O_2^{2-})]^{2+}$ species, and not the $[Cu^{II}(tmpa)(NO_2)]^{+}$ species as expected from $NO_{(g)}$-disproportionation. Elemental analysis confirmed the presence of 2 equiv of both MeOH and water per molecule of the hyponitrito complex: $[\{Cu^{II}(tmpa)\}_2(\mu\text{-}N_2O_2^{2-})][B(C_6F_5)_4]_2.2H_2O.2MeOH$: $C_{86}H_{48}B_2Cu_2F_{40}N_{10}O_6$ calc(%): C 46.40, H 2.17, N 6.29; found (%): C 46.11, H 2.37, N 6.03. In support, the ^1H NMR spectrum of $[\{Cu^{II}(tmpa)\}_2(\mu\text{-}N_2O_2^{2-})]^{2+}$ clearly confirm the presence of MeOH and water (Figure S2). However, the broadness of the water peak at 1.56 delta precludes any reliable use of integrations to determine the ratio of MeOH and water by ^1H NMR spectroscopy. Thus, elemental analysis was used to determine the final formulation.

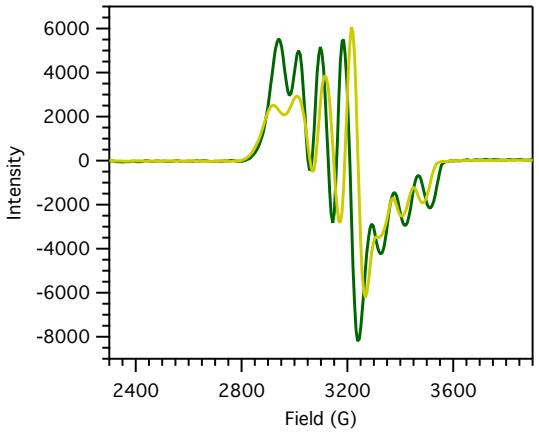

Figure S1. Perpendicular mode EPR spectral comparison between 0.35 mM frozen solution samples of $[Cu^{II}(tmpa)(NO_2)]^{+}$ (olive green) and $[\{Cu^{II}(tmpa)\}_2(\mu\text{-}N_2O_2^{2-})]^{2+}$ (dark green) recorded at 20 K in 1:1 MeOH:EtOH.

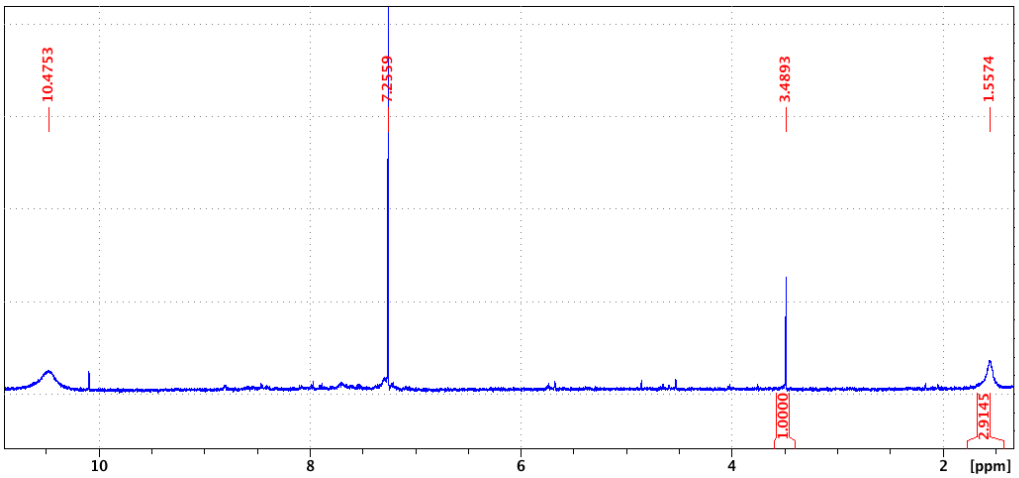

Figure S2. ^{1}H NMR spectrum of $[\{Cu^{II}(tmpa)\}_2(\mu\text{-}N_2O_2^{2-})]^{2+}$ recorded in $CDCl_3$ at room temperature. The 3.48 and 1.56 ppm indicate the presence of MeOH and H_2O, respectively.

3. Titration of $[Cu^{I}(tmpa)(MeCN)]^{+}$ with MeOH-solubilized $NO_{(g)}$

In order to understand the stoichiometry of the reaction between $[Cu^{I}(tmpa)(MeCN)]^{+}$ and nitric oxide in MeOH, a Cu^{I}:$NO_{(g)}$ titration was performed using $NO_{(g)}$-saturated solutions of MeOH. The preparation of such solutions was carried out as follows: A high-pressure purified NO bulb was vented to atmospheric pressure using an inert vent line connected to an oil bubbler, and then MeOH (7 mL) was added into the bulb via a Hamilton gas-tight syringe. This was left to equilibrate for 1hr, and the appropriate amount for each reaction was drawn out using gas-tight syringes. *Note: The bulbs were carefully inspected for NO_2 (a brown-colored gas) formation prior to each use, and were replaced once in every three runs.* The nitric oxide concentration of such $NO_{(g)}$-saturated MeOH solutions are known from previous studies,[10] enabling them to be used as quantitative $NO_{(g)}$ reagents.

Varying volumes (14 – 415 μL) of $NO_{(g)}$-saturated MeOH corresponding to 0.10, 0.25, 0.50, 0.75, 1.00, 2.00, and 3.00 equiv. of $NO_{(g)}$ (with respect to the initial $[Cu^{I}(tmpa)(MeCN)]^{+}$ concentration) was added into 1mM $[Cu^{I}(tmpa)(MeCN)]^{+}$ (2.2 mg, 2×10^{-3} mmol) in MeOH using a gas-tight syringe at room temperature. The volumes of Cu^{I} solutions were pre-adjusted in order to result in 2 mL of 1 mM $[Cu^{I}(tmpa)(MeCN)]^{+}$ in each case following the addition of $NO_{(g)}$. The formation of $[\{Cu^{II}(tmpa)\}_2(\mu\text{-}N_2O_2^{2-})]^{2+}$ was monitored by UV-Vis spectroscopy at 870 nm, and the final yields were calculated from the extinction coefficient (ε_{870} = 340 M^{-1} cm^{-1}) following baseline subtraction at 500 nm (Figure S3 & Table S1). *Note: The charge transfer band of $[\{Cu^{II}(tmpa)\}_2(\mu\text{-}N_2O_2^{2-})]^{2+}$ at 310 nm could not be used to calculate the yields due to the interferences from those of $[Cu^{I}(tmpa)(MeCN)][B(C_6F_5)_4]$ (340 nm).*

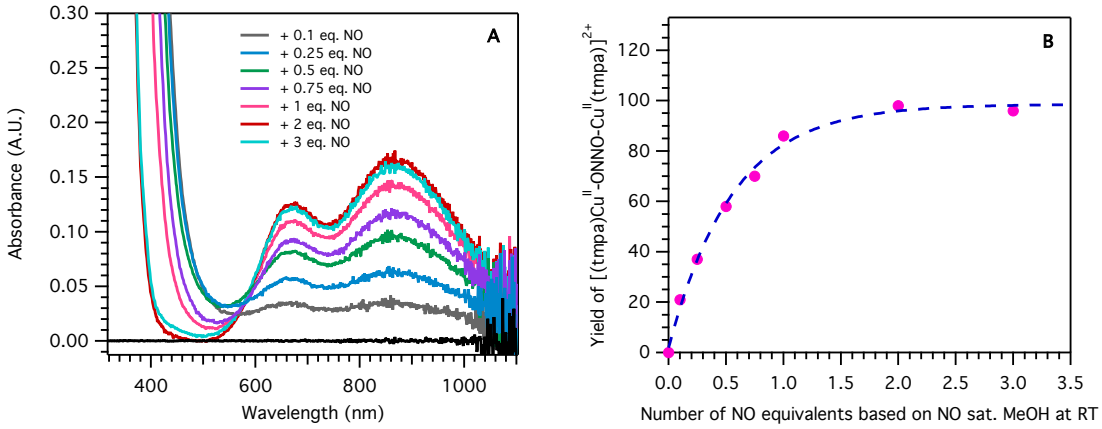

Figure S3. A) Overlay of electronic absorption spectra corresponding to the full formation of $[\{Cu^{II}(tmpa)\}_2(\mu\text{-}N_2O_2^{2-})]^{2+}$ at different equivalents (0.1–3.0) of nitric oxide (with respect to initial $[Cu^{I}]$) in the reaction with $[Cu^{I}(tmpa)(MeCN)]^{+}$ in MeOH at room temperature. Thus, the spectral features in the low-energy visible region increase as shown, until just more than a stoichiometric amount of $NO_{(g)}$ has been added, and the hypontrite complex is fully formed. B) The yields of $[\{Cu^{II}(tmpa)\}_2(\mu\text{-}N_2O_2^{2-})]^{2+}$ corresponding to different $NO_{(g)}$ equivalents added, calculated from the absorption intensities and extinction coefficient at 870 nm.

Table S1. Quantified yields of $[\{Cu^{II}(tmpa)\}_2(\mu\text{-}N_2O_2^{2-})]^{2+}$ at varied $NO_{(g)}$ concentrations (or equivalents) following the reaction between $[Cu^{I}(tmpa)(MeCN)]^{+}$ with nitric oxide at room temperature in MeOH.

Number of $NO_{(g)}$ equiv[a]	Yield[b]
0.10	21%
0.25	37%
0.50	58%
0.75	70%
1.0	86%
2.0	98%
3.0	96%

[a] Number of equivalents based on the starting $[Cu^{I}(tmpa)(MeCN)]^{+}$ concentration. [b] Yield of $[\{Cu^{II}(tmpa)\}_2(\mu\text{-}N_2O_2^{2-})]^{2+}$ is calculated based on absorption maximum at 870 nm (ε_{870} = 340 M^{-1} cm^{-1}).

4. Synthesis of $[\{Cu^{II}(tmpa)\}_2(\mu\text{-}N_2O_2^{2-})]^{2+}$ from $[Cu^{II}(tmpa)(OH)]^{+}$ and *trans*-$Ag_2N_2O_2$

Alternatively, $[\{Cu^{II}(tmpa)\}_2(\mu\text{-}N_2O_2^{2-})]^{2+}$ was synthesized in excellent yields (~96%) via the metathesis reaction between $[Cu^{II}(tmpa)(OH)]^{+}$ and *trans*-$Ag_2N_2O_2$. A solution of

$[Cu^{II}(tmpa)(MeCN)](ClO_4)_2$ (100 mg, 0.17 mmol) was added 1 equiv. of tetrabutylammonium hydroxide (1 M solution in MeOH from Sigma Aldrich) in MeCN (20 mL) under inert atmosphere at ambient temperature. *Note: This reaction has to be carried out under dilute conditions to prevent the decay of* $[Cu^{II}(tmpa)(OH)](ClO_4)$. *Thus, when scaling up, the solvent has to be scaled up accordingly.* The solution color immediately changed from light blue to light green, and the green resultant solution was stirred under Ar for 20 min. This solution was evaporated to dryness under reduced pressure, and the solid residue was redissolved in MeCN, and layered with excess diethyl ether (Figures S4–S6). The resultant green solid was dissolved in MeOH (7 mL) in a 10 mL Schlenk flask, and 0.5 equiv of solid *trans*-$Ag_2N_2O_2$ (23 mg, 0.08 mmol) was added in under reduced light and inert atmosphere. The reaction mixture was then sonicated for ~4 hrs under reduced light conditions. The contents were transferred into the glovebox, and filtered through glass wool to remove the insoluble solid portion. A forest green solution was resulted, which upon drying, produced a forest green solid, which was stable indefinitely at room temperature under inert conditions. This product was characterized by UV-vis and EPR spectroscopies (Figures S7–S8), as well as elemental analysis. Elemental Analysis $[\{Cu^{II}(tmpa)\}_2(\mu\text{-}O^{2-})](ClO_4)_2.2H_2O.2MeOH$: $C_{38}H_{48}Cl_2Cu_2N_8O_{13}$ calc(%): C 44.62, H 4.73, N 10.96; found (%): C 44.71, H 4.01, N 10.24. The observation of the $[\{Cu^{II}(tmpa)\}_2(\mu\text{-}O^{2-})]^{2+}$ complex in elemental analysis suggests that the hyponitrito complex has been thermally decayed during the analysis, giving $N_2O_{(g)}$. Similar decay pathways have been commonly observed for other metal-hyponitrito adducts found in literature (see Wright, A. M. *et al.*, *Inorg. Chem.*, **2015**, *54*, 9330, and references therein; Xu, N. *et al.*, *Nitric Oxide*, **2016**, *52*, 16).

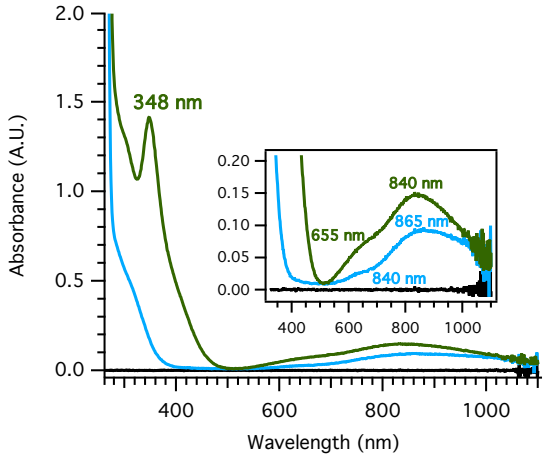

Figure S4. Electronic absorption spectral comparison between 0.4 mM solutions of $[Cu^{II}(tmpa)(MeCN)](ClO_4)_2$ (blue) and $[Cu^{II}(tmpa)(OH)](ClO_4)$ (green) in MeCN at ambient temperature.

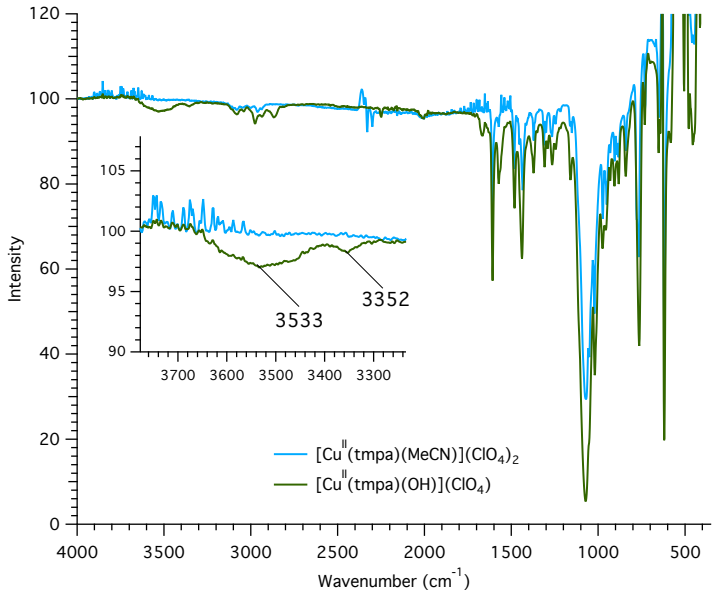

Figure S5. Comparison of solid-state FT-IR spectral features corresponding to $[Cu^{II}(tmpa)(MeCN)](ClO_4)_2$ and $[Cu^{II}(tmpa)(OH)](ClO_4)$ under ambient conditions.

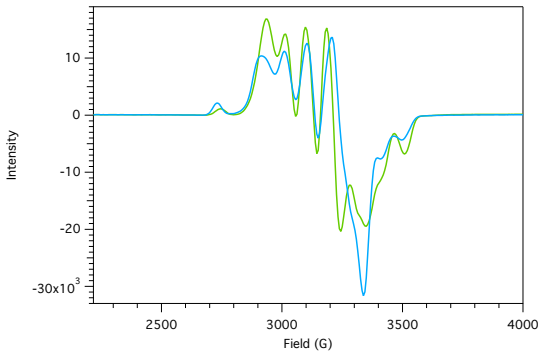

Figure S6. Comparison of perpendicular mode EPR spectra of 2 mM $[Cu^{II}(tmpa)(MeCN)](ClO_4)_2$ (blue) and $[Cu^{II}(tmpa)(OH)](ClO_4)$ (green) recorded at 20 K in frozen MeOH:EtOH 1:1 glass.

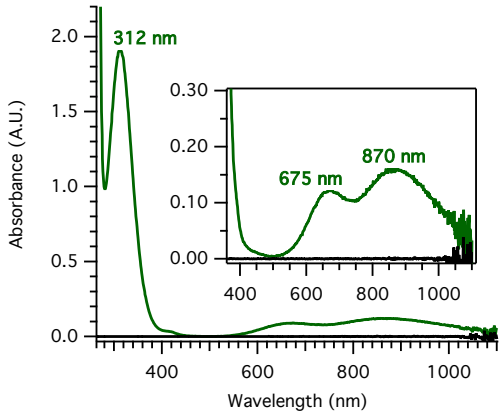

Figure S7. Electronic absorption spectrum of a 0.5 mM methanolic solution (at RT) of $[\{Cu^{II}(tmpa)\}_2(\mu\text{-}N_2O_2^{2-})]^{2+}$ generated from $[Cu^{II}(tmpa)(OH)](ClO_4)$.

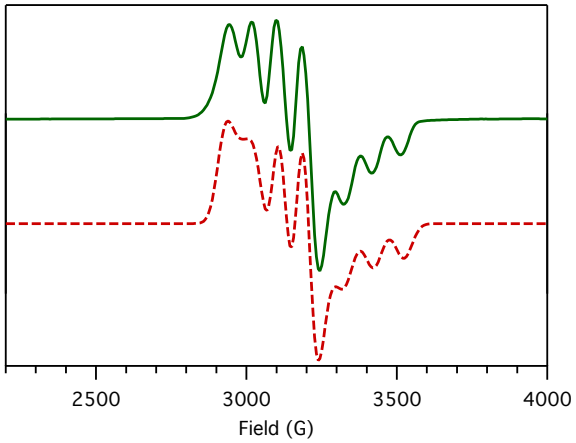

Figure S8. Experimental (green) and simulated (red) EPR spectra of $[\{Cu^{II}(tmpa)\}_2(\mu\text{-}N_2O_2^{2-})]^{2+}$ generated from $[Cu^{II}(tmpa)(OH)](ClO_4)$ (2mM in MeOH/EtOH = 1:1 glass) at 20 K ($g_\perp = 2.18$, $g_\parallel = 1.99$; $A_\perp = 71$ G, $A_\parallel = 95$ G).

5. X-ray diffraction data collection for $[\{Cu^{II}(tmpa)\}_2(\mu\text{-}N_2O_2^{2-})]^{2+}$

X-ray quality crystals of $[\{Cu^{II}(tmpa)\}_2(\mu\text{-}N_2O_2^{2-})](ClO_4)_2$ were obtained from a saturated methanolic solution at -35 ^{O}C over three weeks. This specific sample of $[\{Cu^{II}(tmpa)\}_2(\mu\text{-}N_2O_2^{2-})](ClO_4)_2$ was generated by the metathesis reaction between $[Cu^{II}(tmpa)(Cl)](ClO_4)$ and *trans*-$Ag_2N_2O_2$ following an identical procedure to that described above for the reaction between $[Cu^{II}(tmpa)(OH)](ClO_4)$ and *trans*-$Ag_2N_2O_2$. The crystals exhibited identical spectroscopic signatures to those samples generated by the $[Cu^{I}(tmpa)(MeCN)]^+$ and $NO_{(g)}$ and $[Cu^{II}(tmpa)(OH)](ClO_4)$ and *trans*-$Ag_2N_2O_2$ methodologies described above.

All reflection intensities were measured at 110(2) K using a SuperNova diffractometer (equipped with Atlas detector) with Cu *K*α radiation (λ = 1.54178 Å) under the program CrysAlisPro (Version 1.171.36.32 Agilent Technologies, 2013). The same program was used to refine the cell dimensions and for data reduction. The structure was solved with the program SHELXS-2014/7 (Sheldrick, 2015) and was refined on F^2 with SHELXL-2014/7 (Sheldrick, 2015). Analytical numeric absorption correction based on a multifaceted crystal model was applied using CrysAlisPro. The temperature of the data collection was controlled using the system Cryojet (manufactured by Oxford Instruments). The H atoms were placed at calculated positions using the instructions AFIX 23 or AFIX 43 with isotropic displacement parameters having values 1.2 *U*eq of the attached C atoms.

The asymmetric unit contains one ordered half of the Cu–O–N=N–O–Cu complex (as the complex is found at sites of inversion symmetry) and two disordered perchlorate counterions (one counterion is found at sites of threefold axial symmetry while the other counterion is found at no special position). Four free variables were used to refine the occupancy factors of all components of the disordered counterions, and their values are 0.491(2), 0.204(2), 0.1651(19) and 0.1393(19). The SUMP instruction was used to constrain the sum of the four occupancy factors to be equal to 1 as the charge balance must be neutral. The crystal lattice also contains some small amount of lattice disordered solvent molecules (probably methanol), whose contribution has been taken out in the final refinement (SQUEEZE details are provided in the CIF file, Spek, 2009). *Additional note: prior to the final refinement, the occupancy factors for O1 and N5 were allowed to refine freely, and their refined values were 1.014(7) and 1.017(9), respectively. In the final refinement, those occupancy factors were set to 1.*

Table S2. Selected bond lengths and angles for $[\{Cu^{II}(tmpa)\}_2(\mu\text{-}N_2O_2^{2-})]^{2+}$

Bond	Value	Angle	Value
Cu1–O1	1.9114(14) Å	N3–Cu1–N4	113.81(7)°
Cu1–N1	2.0304(19) Å	N4–Cu1–N1	99.21(7)°
Cu1–N2	2.0575(17) Å	N3–Cu1–N1	140.20(7)°
Cu1–N3	2.0231(19) Å	N2–Cu1–O1	174.58(7)°
Cu1–N4	2.1499(17) Å	N3–Cu1–N2	81.07(7)°
O1–N5	1.361(2) Å	N4–Cu1–N2	80.75(7)°
N5–N5’	1.257(3) Å	N1–Cu1–N2	83.09(7)°
Cu1–N5’	2.851(2) Å	Cu1–O1–N5	120.53(11)°
Cu1–Cu1’	5.5648(7) Å	O1–N5–N5’	112.23(19)°

This following information and arguments strongly support the view that the hyponitrite N_{distal} atom possesses an interaction with the Cu(II) ions in the structure of $[\{Cu^{II}(tmpa)\}_2(\mu\text{-}N_2O_2^{2-})]^{2+}$:

Careful examination of the structural properties of the hyponitrite complex further supports our presumption of each copper center weakly interacting with the distal N atom of the hyponitrite ligand ($Cu–N_{distal}(N5') = 2.851$ Å), as mentioned in the main text. The main points are as follows: Firstly, when comparing the $Cu–N_{ligand}$ distances, the Cu−N4 bond length, which would be *trans* to such an interaction, is the weakest/longest Cu−N bond, where Cu–N4 = 2.15 Å (see Table S2).

Secondly, assuming a pentacoordinate geometry around each copper(II) center (i.e., excluding the $Cu–N_{distal}$ interaction), a geometry index ($\boldsymbol{\tau}$) of 0.57 could be calculated from the solid-state structure of $[\{Cu^{II}(tmpa)\}_2(\mu\text{-}N_2O_2^{2-})]^{2+}$. This stands in sheer contrast to other pentacoordinate Cu(II) complexes supported by the same TMPA ligand platform, where perfect (or near perfect) trigonal bipyramidal (TBP) geometries are observed around the copper center with the $\boldsymbol{\tau}$ value ranging between 0.96 and 1.00.[11] In other words, the fact that this hyponitrite complex does not possess a geometry anywhere close to TBP is indicative of the $Cu\text{-}N_{distal}$ interaction.

Thirdly, in solid-state structures where metal–N_{distal}-type interactions are clearly absent, extended metal-hyponitrite adducts are resulted with much longer metal–N_{distal} and metal–metal interactions[12] (see reference 12; for $[(OEP)Fe^{III}\text{-}ONNO\text{-}Fe^{III}(OEP)]$ (OEP = octaethylporphyrinate), $Fe–N_{distal}$ = 5.062 Å and Fe–Fe = 6.694 Å).

6. Decay studies on $[\{Cu^{II}(tmpa)\}_2(\mu\text{-}N_2O_2^{2-})]^{2+}$ in MeOH:THF 1:19

In aprotic solvents, $[\{Cu^{II}(tmpa)\}_2(\mu\text{-}N_2O_2^{2-})]^{2+}$ was observed to decay with distinct color changes over the course of few hours. To analyze this decay process by electronic absorption, $[\{Cu^{II}(tmpa)\}_2(\mu\text{-}N_2O_2^{2-})]^{2+}$ (0.7 mg, 7×10^{-4} mmol) was dissolved in 100 μL of MeOH, and was placed in a 10 mm Schlenk cuvette. This was then placed in the spectrometer, and THF (1.9 mL) was added in by means of a gas tight syringe, and data collection was initiated immediately. The final concentration of $[\{Cu^{II}(tmpa)\}_2(\mu\text{-}N_2O_2^{2-})]^{2+}$ after the addition of THF was 0.35 mM. The full decay process completed within ~8 hrs (see Figures S9–S10). Samples for product characterization and quantification of this decay reaction were prepared as described below.

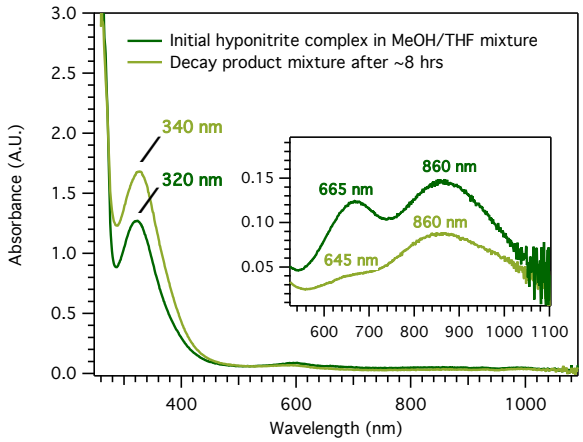

Figure S9. Electronic absorption spectral comparison between the initial and final spectra corresponding to the decay of a 0.35 mM $[\{Cu^{II}(tmpa)\}_2(\mu\text{-}N_2O_2^{2-})]^{2+}$ solution in MeOH:THF 1:19 mixture at room temperature. Note: All absorption features corresponding to the hyponitrite complex in this solvent mixture (prior to its decay; dark green trace above) is ~10 nm shifted from those in pure MeOH (compare with Figure 2 in main text). Furthermore, the final decay products mixture consists of 2:1 $[Cu^{I}(tmpa)]^{+}$ and $[Cu^{II}(tmpa)(NO_2)]^{+}$ (see Figure 1 or Scheme 1). It is noteworthy that both of these compounds have charge transfer features within 300 – 420 nm region, however, the charge transfer band corresponding to $[Cu^{I}(tmpa)]^{+}$ (330 nm; ε = 10, 000 M^{-1} cm^{-1})[13] is of much greater intensity than that of the $[Cu^{II}(tmpa)(NO_2)]^{+}$ (420 nm, ε = 1340 M^{-1} cm^{-1}).[6] Thus, the high energy region of the absorption spectrum of the final decay products strongly resembles that of $[Cu^{I}(tmpa)]^{+}$, rather than $[Cu^{II}(tmpa)(NO_2)]^{+}$. However, since $[Cu^{I}(tmpa)]^{+}$ does not contain any d-d bands, the low energy visible region of the final absorption spectrum is dominated by d-d features corresponding to $[Cu^{II}(tmpa)(NO_2)]^{+}$ (Figure S9 above; light green trace).

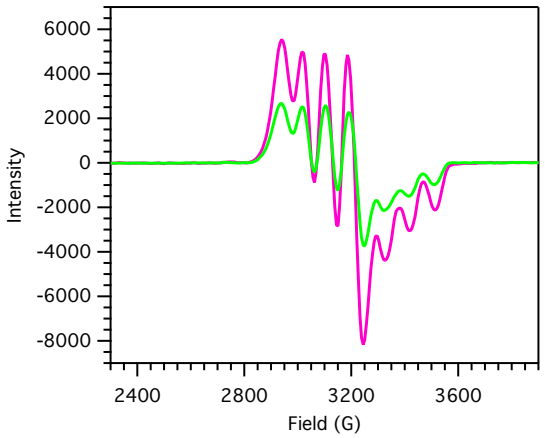

Figure S10. EPR spectral features of $[\{Cu^{II}(tmpa)\}_2(\mu\text{-}N_2O_2^{2-})]^{2+}$ in frozen MeOH:THF 1:19 mixture immediately after mixing in THF (pink), compared with that of the final decay products mixture (green). Both EPR spectra were collected on a 0.35 mM frozen sample at 20 K.

7. Characterization and quantification of decay products of $[\{Cu^{II}(tmpa)\}_2(\mu\text{-}N_2O_2^{2-})]^{2+}$

Cu^{I} Quantification: For this procedure, $[\{Cu^{II}(tmpa)\}_2(\mu\text{-}N_2O_2^{2-})]^{2+}$ (0.2 mg, 2×10^{-4} mmol) was added into a 10 mm path length quartz Schlenk cuvette in 100 μL of MeOH. The cuvette was then sealed with a pierceable rubber septum, and was added 1.9 mL of THF through the septum. The final concentration of $[\{Cu^{II}(tmpa)\}_2(\mu\text{-}N_2O_2^{2-})]^{2+}$ was ~0.15 mM. *Note: The impaired solubility of the perchlorate salt of the hyponitrite complex in THF led us to the utilization of this solvent mixture (i.e., 19:1 THF:MeOH) for all decay studies described here.* The cuvette was left inside the glovebox for overnight decay. It was then transferred into a temperature-controlled cryostat held at -80 °C, and was allowed to obtain thermal equilibrium (10 min). The data collection was then initiated, and dioxygen was bubbled into the final decay product mixture at -80 °C. Characteristic absorption features corresponding to $[\{Cu^{II}(tmpa)\}_2(\mu\text{-}O_2^{2-})]^{2+}$ were immediately generated,[13] indicating the presence of $[Cu^{I}(tmpa)]^{+}$ in the final decay mixture of $[\{Cu^{II}(tmpa)\}_2(\mu\text{-}N_2O_2^{2-})]^{2+}$ (Figure S11). The yield of $[Cu^{I}(tmpa)]^{+}$ was calculated using the extinction coefficient of $[\{Cu^{II}(tmpa)\}_2(\mu\text{-}O_2^{2-})]^{2+}$ at 520 nm (ε_{520} = 14 700 M^{-1} cm^{-1}) under identical experimental conditions. Each experiment was repeated three times for better accuracy.

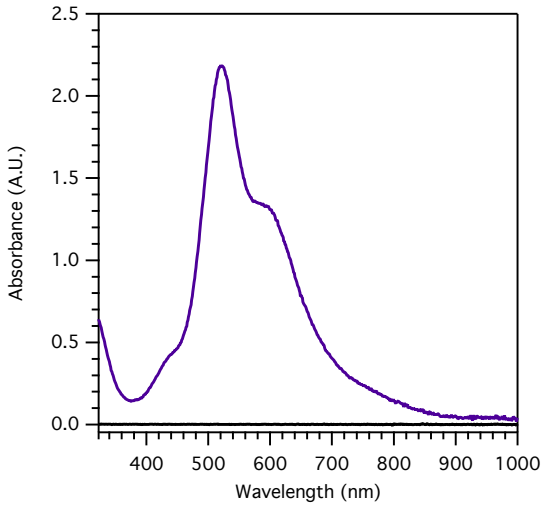

Figure S11. Characteristic optical features corresponding to $[\{Cu^{II}(tmpa)\}_2(\mu\text{-}O_2^{2-})]^{2+}$ formed following the oxygenation of a fully decayed 0.16 mM MeOH:THF 1:19 solution of $[\{Cu^{II}(tmpa)\}_2(\mu\text{-}N_2O_2^{2-})]^{2+}$ at -80 °C.

Nitrite (NO_2^-) Quantification: The quantification of nitrite anion concentration was performed using semi-quantitative QUANTOFIX nitrite test strips. This experiment was designed to produce a $[NO_2^-]$ ~30 mg/L at the end of the full decay of $[\{Cu^{II}(tmpa)\}_2(\mu\text{-}N_2O_2^{2-})]^{2+}$, and each experiment was carried out in triplicate. The detailed procedure is as follows: $[\{Cu^{II}(tmpa)\}_2(\mu\text{-}N_2O_2^{2-})]^{2+}$ (4.7 mg, 4.9×10^{-3} mmol) was allowed to decay in

a sealed ~8 mL clear Wheaton vial overnight. The contents were then transferred into a 10 mL Schelnk flask, and were dried under reduced pressure. The solid residue was redissolved in DCM (3 mL), and was extracted with three 3 mL portions of a 7 mM aqueous NaCl solution. The combined aqueous layer was analyzed with test strips for the quantity of free nitrite. The expected intensity of magenta color was developed, indicating the presence of NO_2^-. In order to confirm the absence of nitrate (NO_3^-) ions, the same sample was treated with excess sulfamic acid, and was retested, which produced negative results at all instances.

$N_2O_{(g)}$ Quantification: The hyponitrito complex, $[\{Cu^{II}(tmpa)\}_2(\mu\text{-}N_2O_2^{2-})]^{2+}$ (7.9 mg, 8×10^{-3} mmol), was placed in a ~8 mL clear Wheaton vial in 100 µL of MeOH. The exact volume of the vial was previously measured (actual volumes varied within 8.1 – 8.5 mL), and was taken into account for final $N_2O_{(g)}$ quantification. The vial was sealed inside the glovebox, and 1.9 mL of THF was syringed in, and the mixture was let to sit overnight at room temperature in the glovebox for complete decay. The green solution gradually turned yellow, which further changed to olive-green upon decaying overnight. In order to quantify the $N_2O_{(g)}$ liberated during this decay, hyponitrous acid ($H_2N_2O_2$) solutions (2.5 mM) were prepared under an inert atmosphere as previously reported.[14] According to this procedure, $Ag_2N_2O_2$ (5.0 mg, 0.02 mmol) was added into a ~8 mL clear Wheaton vial in dark, along with 2 mL of 1:19 MeOH:THF in the glovebox. The vial was sealed, and 5 µL of 2 M HCl (in ether; from Sigma Aldrich) was added using a gas-tight syringe while maintaining reduced light conditions. Immediate formation of a white precipitate was observed, and the solutions were let to decay overnight in dark. For GC analysis, 60 µL of headspace was sampled from each vial, and injected using a 100 µL gas-tight syringe with a sample lock. Triplicate injections were performed with ~1 min intervals, and 3 independent samples were analyzed for higher accuracy. $N_2O_{(g)}$ gas eluted at a retention time of ~6.5 min (Figure S12), and the quantification was effected by calculating the chromatographic peak area while taking into account the headspace volume of the corresponding vial.

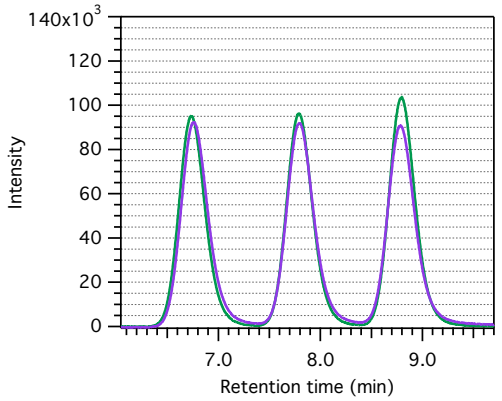

Figure S12. Gas chromatographic comparison of three consecutive injections from the headspace of a fully decayed 4.1 mM MeOH:THF 1:19 solution of $[\{Cu^{II}(tmpa)\}_2(\mu\text{-}N_2O_2^{2-})]^{2+}$ (purple), with those of a equimolar $H_2N_2O_2$ standard in same solvent mixture at room temperature (green).

Table S3. Quantified yields of products resulting from the decay of $[\{Cu^{II}(tmpa)\}_2(\mu\text{-}N_2O_2^{2-})]^{2+}$ in 1:19 MeOH:THF at RT.

Method of Synthesis	Decay Product	Expected molar ratio[a]	Yield Found
Metathesis with *trans*-$Ag_2N_2O_2$	$[Cu^{I}(tmpa)]^{+}$	2/3	96%
	NO_2^-	1/3	>85%
	$N_2O_{(g)}$	1/3	98%
Reductive coupling of $NO_{(g)}$	$[Cu^{I}(tmpa)]^{+}$	2/3	99%
	NO_2^-	1/3	>85%
	$N_2O_{(g)}$	1/3	85%

[a] Stoichiometry based on Cu^{I}-mediated $NO_{(g)}$-disproportionation chemistry, calculated with respect to the starting $[Cu^{I}(tmpa)]^{+}$ concentration.

8. Reactivity of $[\{Cu^{II}(tmpa)\}_2(\mu\text{-}N_2O_2^{2-})]^{2+}$ with 2 equiv of HCl

A methanolic solution (2 mL) of the hyponitrito complex, $[\{Cu^{II}(tmpa)\}_2(\mu\text{-}N_2O_2^{2-})]^{2+}$ (2.1 mg, 1×10^{-3} mmol) was placed in a 10 mm path length quartz Schlenk cuvette, and data collection was initiated at RT. Then, 2 equiv of HCl (using a 2 M solution in ether; from Sigma Aldrich) was added in under inert conditions using a Hamilton gas-tight syringe. An immediate color change from forest green to blue was observed, and the related electronic absorption spectral changes are summarized in Figure S13. This reaction was repeated in a ~8 mL clear Wheaton vial in MeOH at identical concentrations described above for the quantification of $N_2O_{(g)}$ by gas chromatography (see Page S13). The headspace was sampled using GC, and compared to that of a $H_2N_2O_2$ standard as mentioned above (Figure S14). The resultant $[Cu^{II}(tmpa)(Cl)]^{+}$ complex (identified and quantified by comparison to the UV-vis of an authentic standard compound (Figure S13; also see ref. 15 of the main text) and $N_2O_{(g)}$ (Figure S14) were observed in ~85 % and ~70 % yields respectively.

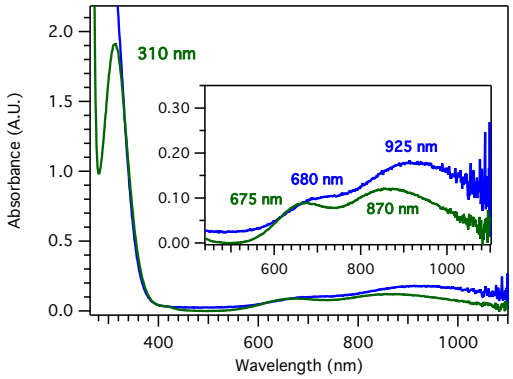

Figure S13. Electronic absorption spectral changes observed as a 0.5 mM methanolic solution of $[\{Cu^{II}(tmpa)\}_2(\mu\text{-}N_2O_2^{2-})]^{2+}$ is reacted with 2 equiv of HCl at RT.

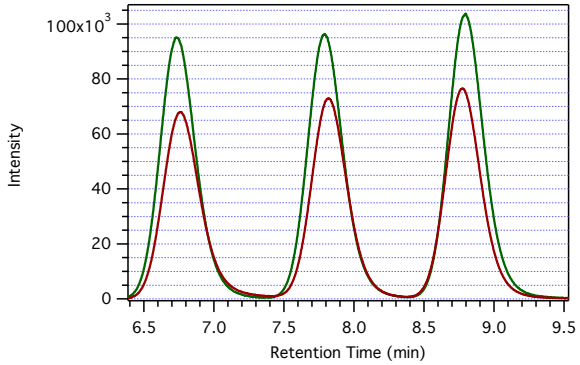

Figure S14. Gas chromatographic comparison between the headspace of a fully reacted methanolic solution of $[\{Cu^{II}(tmpa)\}_2(\mu\text{-}N_2O_2^{2-})]^{2+}$ with 2 equiv of HCl (maroon), and a fully decayed equimolar $H_2N_2O_2$ standard solution (green) at room temperature.

9. Reactivity of $[Cu^{I}(tmpa)(MeCN)]^{+}$ with excess $NO_{(g)}$ in THF leading to $NO_{(g)}$-disproportionation

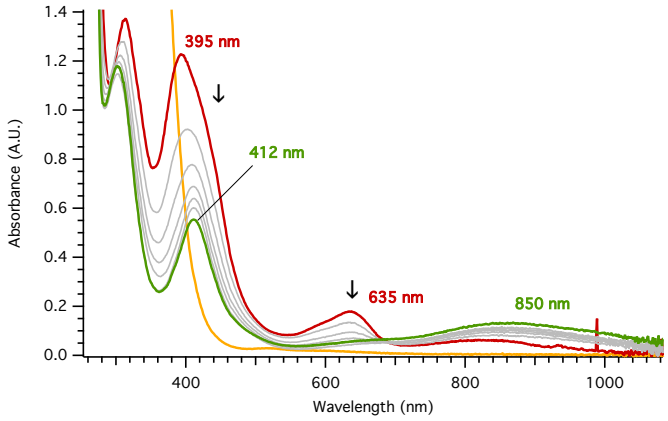

Figure S15. Electronic absorption spectra collected as a 0.3 mM $[Cu^{I}(tmpa)(MeCN)]^{+}$ solution disproportionates excess $NO_{(g)}$ in THF at –80 °C. As $[Cu^{I}(tmpa)(MeCN)]^{+}$ (orange) reacts with excess with nitric oxide, an immediate formation of an distinct initial intermediate is observed (dark red), which then gradually transforms into $[Cu^{II}(tmpa)(NO_2)]^{+}$. The final yield of $[Cu^{II}(tmpa)(NO_2)]^{+}$ (96 %) was calculated using its extinction coefficient at 412 nm (under identical conditions), and the starting Cu^{I} concentration.

References

(1) Schopfer, M. P.; Mondal, B.; Lee, D.-H.; Sarjeant, A. A. N.; Karlin, K. D. *J. Am. Chem. Soc.* **2009**, *131*, 11304.

(2) Ford, P. C.; Lorkovic, I. M. *Chem. Rev. (Washington, DC, U. S.)* **2002**, *102*, 993.

(3) Wang, J.; Schopfer, M. P.; Sarjeant, A. A. N.; Karlin, K. D. *J. Am. Chem. Soc.* **2009**, *131*, 450.
(4) Jacobson, R. R.; Tyeklar, Z.; Farooq, A.; Karlin, K. D.; Liu, S.; Zubieta, J. *J. Am. Chem. Soc.* **1988**, *110*, 3690.
(5) Liang, H.-C.; Kim, E.; Incarvito, C. D.; Rheingold, A. L.; Karlin, K. D. *Inorg. Chem.* **2002**, *41*, 2209.
(6) Hematian, S.; Siegler, M. A.; Karlin, K. D. *J. Am. Chem. Soc.* **2012**, *134*, 18912.
(7) Fox, S.; Nanthakumar, A.; Wikström, M.; Karlin, K. D.; Blackburn, N. J. *J. Am. Chem. Soc.* **1996**, *118*, 24.
(8) Arulsamy, N.; Bohle, D. S.; Imonigie, J. A.; Sagan, E. S. *Inorg. Chem.* **1999**, *38*, 2716.
(9) Wasser, I. M.; de Vries, S.; Moënne-Loccoz, P.; Schröder, I.; Karlin, K. D. *Chem. Rev. (Washington, DC, U. S.)* **2002**, *102*, 1201.
(10) Lim, M. D.; Lorković, I. M.; Ford, P. C. *Methods Enzymol.* **2005**, *396*, 3.
(11) Lee, Y.; Park, G. Y.; Lucas, H. R.; Vajda, P. L.; Kamaraj, K.; Vance, M. A.; Milligan, A. E.; Woertink, J. S.; Siegler, M. A.; Narducci Sarjeant, A. A.; Zakharov, L. N.; Rheingold, A. L.; Solomon, E. I.; Karlin, K. D. *Inorg. Chem.* **2009**, *48*, 11297.
(12) Xu, N.; Campbell, A. L. O.; Powell, D. R.; Khandogin, J.; Richter-Addo, G. B. *J. Am. Chem. Soc.* **2009**, *131*, 2460.
(13) Tyeklar, Z.; Jacobson, R. R.; Wei, N.; Murthy, N. N.; Zubieta, J.; Karlin, K. D. *J. Am. Chem. Soc.* **1993**, *115*, 2677.
(14) Arulsamy, N.; Bohle, D. S.; Imonigie, J. A.; Sagan, E. S. *J. Am. Chem. Soc.* **2000**, *122*, 5539.